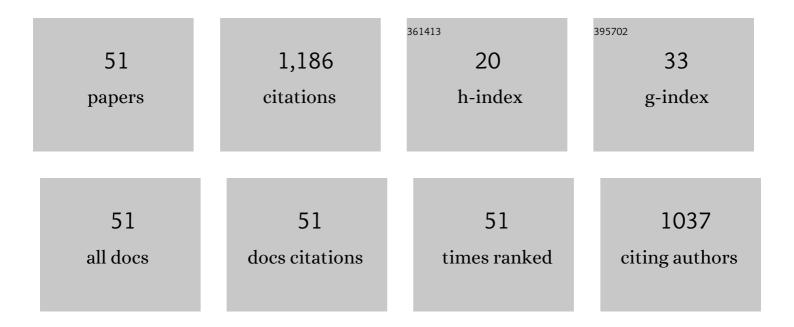
Jinbo Xue

List of Publications by Year in descending order

Source: https://exaly.com/author-pdf/7191859/publications.pdf Version: 2024-02-01



#	Article	IF	CITATIONS
1	Self-Doping Surface Oxygen Vacancy-Induced Lattice Strains for Enhancing Visible Light-Driven Photocatalytic H ₂ Evolution over Black TiO ₂ . ACS Applied Materials & Interfaces, 2021, 13, 18758-18771.	8.0	127
2	Oxygen vacancy self-doped black TiO2 nanotube arrays by aluminothermic reduction for photocatalytic CO2 reduction under visible light illumination. Journal of CO2 Utilization, 2020, 35, 205-215.	6.8	116
3	A C@TiO ₂ yolk–shell heterostructure for synchronous photothermal–photocatalytic degradation of organic pollutants. Journal of Materials Chemistry C, 2020, 8, 1025-1040.	5.5	71
4	Construction of CdSe polymorphic junctions with coherent interface for enhanced photoelectrocatalytic hydrogen generation. Applied Catalysis B: Environmental, 2021, 282, 119552.	20.2	69
5	Construction of a ternary spatial junction in yolk–shell nanoreactor for efficient photo-thermal catalytic hydrogen generation. Chemical Engineering Journal, 2021, 423, 130188.	12.7	54
6	MIL-100 (Fe) with mix-valence coordinatively unsaturated metal site as Fenton-like catalyst for efficiently removing tetracycline hydrochloride: Boosting Fe(III)/Fe(II) cycle by photoreduction. Separation and Purification Technology, 2021, 262, 118334.	7.9	47
7	3D hierarchically porous NiO/NF electrode for the removal of chromium(VI) from wastewater by electrocoagulation. Chemical Engineering Journal, 2020, 402, 126151.	12.7	46
8	Black single-crystal TiO2 nanosheet array films with oxygen vacancy on {001} facets for boosting photocatalytic CO2 reduction. Journal of Alloys and Compounds, 2021, 870, 159400.	5.5	42
9	A promoted photocatalysis system trade-off between thermodynamic and kinetic via hierarchical distribution dual-defects for efficient H2 evolution. Chemical Engineering Journal, 2022, 431, 133281.	12.7	41
10	Assisting Bi2MoO6 microspheres with phenolic resin-based ACSs as attractive tailor-made supporter for highly-efficient photocatalytic CO2 reduction. Green Energy and Environment, 2021, 6, 693-702.	8.7	38
11	Photosensitization of TiO2 nanotube arrays with CdSe nanoparticles and their photoelectrochemical performance under visible light. Electrochimica Acta, 2013, 97, 10-16.	5.2	34
12	The dual effects of RGO films in TiO2/CdSe heterojunction: Enhancing photocatalytic activity and improving photocorrosion resistance. Applied Surface Science, 2019, 481, 1515-1523.	6.1	34
13	Preparation and formation mechanism of smooth and uniform Cu2O thin films by electrodeposition method. Surface and Coatings Technology, 2013, 216, 166-171.	4.8	33
14	The study on properties of CdS photocatalyst with different ratios of zinc-blende and wurtzite structure. RSC Advances, 2013, 3, 20930.	3.6	27
15	High-performance ordered porous Polypyrrole/ZnO films with improved specific capacitance for supercapacitors. Materials Chemistry and Physics, 2020, 256, 123591.	4.0	26
16	Crystallization behavior and formation mechanism of dendrite Cu2O crystals. CrystEngComm, 2012, 14, 8017.	2.6	24
17	Enhancing efficiency of CdS/TiO2 nanorod arrays solar cell through improving the hydrophilicity of TiO2 nanorod surface. Solar Energy Materials and Solar Cells, 2015, 136, 206-212.	6.2	23
18	A gas bubble exfoliation method to prepare g-C3N4 nanosheets with enhanced photocatalytic activities. Journal of Photochemistry and Photobiology A: Chemistry, 2019, 372, 147-155.	3.9	21

Jinbo Xue

#	Article	IF	CITATIONS
19	Effect of oxygen vacancies on the photocatalytic CO2 reduction performance of Bi2WO6: DFT and experimental studies. Applied Surface Science, 2022, 579, 152135.	6.1	21
20	Investigation on the influence of pH on structure and photoelectrochemical properties of CdSe electrolytically deposited into TiO2 nanotube arrays. Journal of Alloys and Compounds, 2014, 607, 163-168.	5.5	20
21	Three-dimensional porous Cu2O with dendrite for efficient photocatalytic reduction of CO2 under visible light. Applied Surface Science, 2022, 581, 152343.	6.1	18
22	A novel synthesis method for Ag/g-C3N4 nanocomposite and mechanism of enhanced visible-light photocatalytic activity. Journal of Materials Science: Materials in Electronics, 2019, 30, 15636-15645.	2.2	16
23	Enhanced photoelectrocatalytic hydrogen production performance of porous MoS2/PPy/ZnO film under visible light irradiation. International Journal of Hydrogen Energy, 2021, 46, 35219-35229.	7.1	16
24	Shape-controlled synthesis of three-dimensional branched CdS nanostructure arrays: structural characteristics and formation mechanism. CrystEngComm, 2013, 15, 1007-1014.	2.6	15
25	Effects of annealing temperature on the properties of copper films prepared by magnetron sputtering. Journal Wuhan University of Technology, Materials Science Edition, 2015, 30, 92-96.	1.0	14
26	Photoelectrocatalytic hydrogen production of heterogeneous photoelectrodes with different system configurations of CdSe nanoparticles, Au nanocrystals and TiO2 nanotube arrays. International Journal of Hydrogen Energy, 2020, 45, 26688-26700.	7.1	14
27	Performance of photocatalytic cathodic protection of 20 steel by α-Fe2O3/TiO2 system. Surface and Coatings Technology, 2020, 385, 125445.	4.8	14
28	Synthesis of disorder–order TaON homojunction for photocatalytic hydrogen generation under visible light. Journal of Materials Science, 2021, 56, 9791-9806.	3.7	14
29	Controlled synthesis of coaxial core–shell TiO2/Cu2O heterostructures by electrochemical method and their photoelectrochemical properties. Materials Letters, 2013, 92, 239-242.	2.6	13
30	Electrodeposition of Cu2O nanocrystalline on TiO2 nanosheet arrays by chronopotentiometry for improvement of photoelectrochemical properties. Ceramics International, 2018, 44, 11039-11047.	4.8	13
31	A 3D C@TiO2 multishell nanoframe for simultaneous photothermal catalytic hydrogen generation and organic pollutant degradation. Journal of Colloid and Interface Science, 2022, 609, 535-546.	9.4	13
32	In-situ construction of photoanode with Fe2O3/Fe3O4 heterojunction nanotube array to facilitate charge separation for efficient water splitting. Journal of Alloys and Compounds, 2022, 918, 165787.	5.5	13
33	Preparation and enhanced daylight-induced photo-catalytic activity of transparent C-Doped TiO2 thin films. Journal Wuhan University of Technology, Materials Science Edition, 2010, 25, 738-742.	1.0	11
34	Annealing temperature effect on 3D hierarchically porous NiO/Ni for removal of trace hexavalent chromium. Materials Chemistry and Physics, 2020, 240, 122140.	4.0	10
35	In Situ Synthesis of Hydrangea Finch Coral-like Bi ₁₂ SiO ₂₀ Film with Highly Effective Photocatalytic CO ₂ Reduction Performance. ACS Applied Energy Materials, 2021, 4, 15-19.	5.1	10
36	Effect of oxygen vacancy concentration on the photocatalytic hydrogen evolution performance of anatase TiO2: DFT and experimental studies. Journal of Materials Science: Materials in Electronics, 2021, 32, 13369-13381.	2.2	9

Jinbo Xue

#	Article	IF	CITATIONS
37	Construction of an amino-rich Ni/Ti bimetallic MOF composite with expanded light absorption and enhanced carrier separation for efficient photocatalytic H2 evolution. Materials Science in Semiconductor Processing, 2022, 150, 106914.	4.0	9
38	The Oxygen Reduction Reaction Rate of Metallic Nanoparticles during Catalyzed Oxidation. Scientific Reports, 2017, 7, 7017.	3.3	7
39	Electrochemical preparation and photoelectric properties of Cu2O-loaded TiO2 nanotube arrays. Journal Wuhan University of Technology, Materials Science Edition, 2014, 29, 23-28.	1.0	6
40	Microstructure and mechanical properties of ultrafine grained Mg15Al alloy processed by equal-channel angular pressing. Journal Wuhan University of Technology, Materials Science Edition, 2010, 25, 238-242.	1.0	5
41	Facile and time-saving synthesis of octahedral Cu ₂ O crystals by an ethanol-assisted solution method at low temperatures. CrystEngComm, 2017, 19, 1258-1264.	2.6	5
42	Robust Fe2+-doped nickel-iron layered double hydroxide electrode for electrocatalytic reduction of hexavalent chromium by pulsed potential method. Journal of Materials Science and Technology, 2022, 110, 73-83.	10.7	5
43	Influence of annealing temperature on microstructure and photoelectric properties of ternary CdSe@CdS@TiO2 core–shell heterojunctions. Journal of Solid State Electrochemistry, 2019, 23, 2085-2096.	2.5	4
44	{001}/{101} facets co-exposed TiO2 microsheet arrays with Lanthanum doping for enhancing photocatalytic CO2 reduction. Journal of Materials Science: Materials in Electronics, 2020, 31, 19464-19474.	2.2	4
45	Electronic band structures of TiO2 with heavy nitrogen doping. Journal Wuhan University of Technology, Materials Science Edition, 2008, 23, 799-803.	1.0	3
46	Theoretical insights into effective electron transfer and migration behavior for CO ₂ reduction on the BiOBr(001) surfaces. Physical Chemistry Chemical Physics, 2022, 24, 2032-2039.	2.8	3
47	Effect of ECAP on the microstructure and mechanical properties of a high-Mg2Si content Al-Mg-Si alloy. Journal Wuhan University of Technology, Materials Science Edition, 2010, 25, 395-398.	1.0	2
48	The surface wettability of TiO2 nanotube arrays: which is more important—morphology or chemical composition?. Journal of Porous Materials, 2019, 26, 91-98.	2.6	2
49	In-situ growth of MOF nanosheets with controllable thickness on copper foam for photoelectrocatalytic CO2 reduction. Journal of Materials Science: Materials in Electronics, 2022, 33, 14568-14580.	2.2	2
50	The influence of Au nuclei layer on formation and photoelectrochemical properties of Cu2O thin films. Journal of Materials Science: Materials in Electronics, 2017, 28, 8579-8587.	2.2	1
51	The influence of DMSO on the formation and photoelectrochemical properties of CdS thin films by electrodeposition method. Journal of Solid State Electrochemistry, 2017, 21, 19-26.	2.5	1